

## An investigation into the motion and stability behaviour of a RO-RO vessel

Poonam Mohan\* and A.P. Shashikala

*Department of Civil Engineering, National Institute of Technology, Calicut, India*

*(Received November 6, 2018, Revised April 10, 2019, Accepted April 11, 2019)*

**Abstract.** Studies on motion response of a vessel is of great interest to researchers, since a long time. But intensive researches on stability of vessel during motion under dynamic conditions are few. A numerical model of vessel is developed and responses are analyzed in head, beam and quartering sea conditions. Variation of response amplitude operator (RAO) of vessel based on Strip Theory for different wave heights is plotted. Validation of results was done experimentally and numerical results was considered to obtain effect of damping on vessel stability. A scale model ratio of 1:125 was used which is suitable for dimensions of wave flume at National Institute of Technology Calicut. Stability chart are developed based on Mathieu's equation of stability. Ince-Strutt chart developed can help to capture variations of stability with damping.

**Keywords:** in-tact stability; Mathieu's equation; Response Amplitude Operator (RAO)

---

### 1. Introduction

Ships are generally effected by dynamic waves in head, beam and quarter sea condition. During its static condition, fluctuations in self-weight and buoyancy play a major role. Onset of waves contributes to dynamic condition of vessel and then stability conditions vary abruptly along with change in vessel motion. Direction of wave impact and vessel speed influences motion behavior of vessel.

Ro-Ro (Roll-on/roll-off) vessel has a high risks in design due to less number of internal bulkheads (Knapp 1995). It has great stability issues even though this ship proved very useful in terms of speed, cost and time effectiveness. These vessels require proper and careful handling because it has large deck area with transverse bulkheads which promotes rapid inrush of flood water and sudden failure on hull. Also, cargo or passenger movements give rise to unanticipated intact stability loss and listing (Ibrahim and Grace 2010). Huge superstructure of vessel can cause stability loss due to wind. Loading and unloading process require great attention in stability point of view. Due to these reasons, change in GM may make vessel fail to satisfy standard regulatory requirements, leading to collapse of vessel.

By understanding criticality of vessel design, Allianz Global Corporate published a report namely "*Safety and Shipping 1912-2012: from Titanic to Costa Concordia*" from studies done by Cardiff University, which lists casualty in percentage during year 2000-2010 for Cargo Vessels as

---

\*Corresponding author, Research Scholar, E-mail: [poonammohan89@gmail.com](mailto:poonammohan89@gmail.com)

44.5%, Passengers/General Cargo as 5.2% and Passenger Cruise as 1.1%. From this survey, it is understood that problem of motion and stability is to be studied even more intensively in case of Ro-Ro vessel. Many projects were involved in study of variations in motion in intact and damage stability to harmonize Ro-Ro vessels and to keep rules and regulations updated to recent unconventional methods. These includes GOALDS, EMSA III, FLOOD-STAND, HARDER, ROROPROB etc.

Table 1 Nomenclature

Parameters	Unit
Centre of gravity	CG
Aft Perpendicular	AP
Draft at Aft Perpendicular	d
Block coefficient	$C_B$
Prismatic coefficient	$C_P$
Length overall	$L_{OA}$
Length between perpendiculars	$L_{PP}$
Breadth Moulded	b
Midship section coefficient	$C_M$
Roll ,Pitch radius of gyration	$K_{xx}, K_{yy}$
Breadth Moulded	b
Amidships section coefficient	$C_M$
Water plane coefficient	$C_{WP}$
Height of keel to metacenter	KM
Height of keel to C.G	KG
Metacentric height	GM
Longitudinal position of C.G	LCG
Modulus of Elasticity	E
Wavelength	$\lambda$
Wave Frequency	$\omega$
Wave encountering frequency	$\omega_e$
Displacement	$\Delta$
Moment of Inertia about roll axis	$I_4$
Angle of heel	$\phi$
Heave RAO	H
Pitch RAO	P
Damping Coefficient	B
Stiffness Coefficient	C
Damping ratio	$\epsilon$
Damped frequency of oscillation	$\omega_D$
Added mass	A
External Exciting Force	$F_4$
Forward speed	V

The fact that Ro-Ro Vessels are operated at required metacentric height (GM) close to damage stability requirement (Hanzu 2016) leaves a gap for further research in this area. Stability criteria should always be governed by intact stability conditions, rather than damage stability conditions. Fernández (2015) did stability investigation on damaged ships and found that it is more complex phenomenon.

Experimental and numerical investigations have been carried out to estimate motion behavior of vessel. Wave height is varied and type of wave used is small regular waves suitable for model length. Anastopoulos and Spyrou (2016) performed dynamic stability analysis for varying wave group excitations. In present study, model study carried out by Korkut *et al.* (2004) was considered to validate scale model and results were found to be considerably agreeing. Above results were also validated using numerical codes. Stable and unstable region of a partial differential equation like Mathieu's equation is represented by Ince-strut chart. Thus region of stability of vessel can be defined for different wave height and by finding out damping coefficient. Damped Ince Strutt diagram is plotted to observe stability regions for a vessel in dynamic condition.

## 2. Review of related works

Research in motion of vessel is wide and a number of literatures are available to estimate response of ships, while stability assessment during motion is often not focused. To start with, focus is laid on work relating motion response and stability relationships. Moideen and Falzarano (2011) worked in area of parametric rolling considering both regular and irregular sea conditions. They tried to simplify roll equation of motion from six degrees of freedom system by retaining nonlinear properties of system using bounded Ince Strutt Chart. Insperger (2003) analyzed stability of time delayed Damped Mathieu's equation. They developed Strutt Ince and Hsu Bhatt Vyshegradskii chart which reveals stability properties of an oscillatory system undergoing parametric excitation. Ribeiro (2010) observed parametric roll of a container. They suggested best method to study vessel roll behavior as spring-mass system resulting in a relationship between  $\omega_c$  and  $\omega$ . Another method is to represent responses in Mathieu's equation form and to find out instability regions.

Bergdahl (2009) studied wave-induced loads on ship motion in irregular sea state and suggested recommendation on allowable motion in vessel while moored in harbor. Taylan (2004) estimated stability of vessel under motion. Variation of GZ curve at different forward speed was being observed. He found that with increasing speed damping characteristics have greater influence on vessel motion behavior. Begovic *et al.* (2013) performed model test on two scale models and observed that prediction of responses in resonant condition is very complex. They found discrepancies in motion responses due to vortex shedding at bilge keel. Hsiung (1991) did comparison of strip and panel theory to estimate motion response under forward-speed. They concluded that panel method overestimates at low Froude's number for heave and pitch responses at higher Froude's number. Zakaria (2007) studied effects of ship size, speed and wave encountering direction for different wave heights in container vessel. He found that, in rough sea condition, problem of bow slamming and propeller emergence is higher. Blome and Krueger (2003) pointed out requirement of further improving intact and damage stability regulations to demonstrate how safety levels can be accessed especially in rough weather. Studies to prevent resonant stage in operating condition are also few. Acanfora and Fabio (2016) studied effects of flooded ship motions and how flood water moves across damaged hole in three different damage scenarios and obtained its motion responses.

Korkut *et al* (2005) found that roll on-roll off type vessel is susceptible to instability, once they are damaged than all other types of vessel. Motion analysis was done to understand sea keeping behavior. Ship model was tested by varying H and  $\omega$  for head, beam, and quartering seas, thus finding response in damaged condition. Even slight sectional damage was found to show significant variation in damage response which was also highly influenced by wave directionality and frequency range (Francescutto 2015). In present study, a combination of different wave heights and wave frequencies are studied and its effects on motion and stability of Ro-Ro vessel is evaluated.

### 3. Governing equations

#### 3.1 Motion analysis

Strip theory assumes slender hull, low speed 'V', and high encountering frequency. In strip theory under head sea condition heave and pitch attains maximum value (Zakaria 2007). For a ship with 6DOF subjected to high sea state, it undergoes a heave, roll, pitch, surge, sway and yaw motion. Motion equation is influenced by quantities like mass, stiffness and damping coefficients incorporated where, indices 'i' represents degrees of freedom and 'ij' means coupled motion responses (Xia 2002). When  $i = 1, 2, 3$ , they represents surge, sway and heave displacements while  $i=4, 5, 6$  represents roll, pitch, yaw motion of the vessel. Therefore, general equation of system maybe represented as follows

$$[M_{ij}+A_{ij}] \ddot{\phi}_i + [B_{ij}] \dot{\phi}_i + [C_{ij}] \phi_i = [F_i] \quad (1)$$

External excitation is due to encountering waves at an angle ' $\mu$ ', direction of vessel motion and encountering frequency which is given by

$$\omega_e = \omega - (\omega^2 V \cos \mu) / g \quad (2)$$

Analysis include specifying problem under consideration w.r.t parameters like vessel headings, wave type and locations at which motions is to be evaluated. Panel method requires more computation time as it uses Green's theorem. Strip theory is a widely used method for slender ships, significantly predicting dynamic condition of vessel. It assumes that radiation and diffraction terms vary along length of vessel, leading to a simplified formulation hence easy to compute. Table 1 gives nomenclature related to model under study.

#### 3.2 Mathieu stability equation

Uncoupled roll motion may be represented in second order differential equation form as shown in Eq. (3)

$$[I_4+A_{44}] (\ddot{\phi}_4) + [B_{44}](\dot{\phi}_4) + C_{44} (\phi_4) = [F_4] \quad (3)$$

$$\text{Where; } C_{44} = g \cdot \Delta GM \quad (4)$$

Time varying Roll equation is

$$\begin{aligned} C(t) &= \Delta g \cdot GZ(t) \\ \omega_D &= \omega \sqrt{1-\varepsilon^2} \end{aligned} \quad (5)$$

Roll frequency is  $\omega_{44}$  and initial metacentric height is  $GM_0$ . Then higher order linearized equation becomes

$$\ddot{\phi}_4 + \left[ \frac{B\omega_{44}}{(I+A\omega_{44})\omega} \right] \dot{\phi}_4 + \left[ \frac{g\Delta GM_0}{(I+A\omega_{44})\omega} \right] + \left[ \frac{g\Delta GM \cos \omega t}{(I+A\omega_{44})\omega} \right] (\phi_4) = 0 \tag{6}$$

Where,

- $\ddot{\phi}_4$  – Roll acceleration  $\Delta GM_0$  – Change in metacentric height at static condition
- B – Damping coefficient  $\Delta GM$  -Change in metacentric height at dynamic condition
- $\omega_{44}$  – Frequency of roll motion  $\Phi_4$  – Roll angle of motion
- I – Moment of inertia in roll  $\dot{\phi}$  - Roll angular velocity
- A – Added mass in roll  $\omega$  - Frequency of wave
- g – Acceleration due to gravity

This is of the form of Mathieu’s equation.

$$\frac{d^2\phi}{dz^2} + \mu \frac{d\phi}{dz} + (\alpha + Y \cos n \tau)\phi = 0 \tag{7}$$

$$\phi = a_0 + \sum_{n=1}^{\infty} (a_n \cos n\tau + b_n \sin n\tau) \tag{8}$$

Here  $\alpha$ ,  $Y$ , defines boundaries of stability region. Coefficients  $a_0$ ,  $a_n$ ,  $b_n$  are Fourier transform coefficients. Thus from comparing Eqs. (6) and (7), transformation constants required to develop stability chart may be obtained.

$$n\tau = n\omega t = n(2\pi)t/T \tag{9}$$

where, period  $T = \pi, 2\pi, 3\pi, \dots, n\pi$  and  $n = 1, 2, 3, \dots, \infty$ . Therefore,  $\tau = t/2, t, 3t/2, 2t, \dots, \infty$ . Substituting, above conditions in Eq. (8), we get a set of equations, which when represented in matrix form is as shown in Section 7. Determinant of coefficient matrix is set to zero and resulting plot gives Ince-Strutt chart.

### 3.3 Undamped

Allievi and Soudack (1990) formulated relationship between ship stability and its response using series expansion with reference to Kerwin (1995). They considered a freely floating body where displaced weight acts downward through center of gravity CG and buoyant force acting upward through center of buoyancy, opposite in sign. Vessel heel at a heel angle of ‘ $\phi$ ’ and metacenter is ‘M’. Center of gravity and Centre of buoyancy is separated by a distance G. Righting moment was calculated when vessel is subjected to head sea condition. When pitch, surge, and heave occur and then the respective GM value changes as ‘M’ start to change and takes encountering period. Fluctuation in righting moment occurs when sinusoidal waves move along different hull sections of vessel. Hill’s Equation is represented as

$$\ddot{\phi} + h(t)\phi = 0 \tag{10}$$

If wave is of cosine form, then assuming stiffness coefficient,  $h(t) = (\alpha + Y \cos n \tau)$ , we get Mathieu’s equation

$$\ddot{\phi} + (\alpha + Y \cos n \tau)\phi = 0 \tag{11}$$

Where, 
$$\alpha = \frac{\omega^2}{\omega_e^2}, c = \frac{\Delta GM}{2GM}, \gamma = \frac{\Delta GM}{4GM} * \frac{\omega^2}{\omega_e^2} = \frac{c}{2} * \alpha \quad (12)$$

$$\ddot{\phi} + \left[ \frac{\omega^2}{\omega_e^2} + \frac{\Delta GM}{4GM} * \frac{\omega^2}{\omega_e^2} \cos n\tau \right] \phi = 0 \quad (13)$$

This gives relation between angle of heel and metacentric height.

### 3.4 Uncertainty analysis

For measurement of uncertainty of wave amplitude using wave probes Eq. (14) is used. Here, suffix p, t represents crest and trough of wave.

$$A = (a_p - a_t)/2 \quad (14)$$

Bias error includes scale effect, modelling issues, test set up errors, calibration error, wave generator error and wall effect. Error components includes bias limits (B) and precision index which are measured using following equations

$$B_a = \left( \frac{\partial a}{\partial a_p} B a_p \right)^2 + \left( \frac{\partial a}{\partial a_t} B a_t \right)^2 + \left( 2\rho_{pt} \frac{\partial a}{\partial a_p} \frac{\partial a}{\partial a_t} B a_p B a_t \right) \quad (15)$$

Error of measuring devices is obtained from calibration and is represented as Standard Error of Estimate (SEE) index given by Eq. (15).

$$SEE^2 = \frac{1}{N-V} \sum_{k=1}^N (y_k - y_{f,k})^2 \quad (16)$$

Where, N is number of data used for calibration, V is number of variable used for fitting,  $y_k$  is data used and  $y_{f,k}$  fitting value for data. For motion analysis heave (H) and pitch (P) ratio, bias limits, precision index (p) and uncertainty ( $U_H$ ) is measured by following equation:

For Heave;

$$\left. \begin{aligned} H' &= H/a \\ B_H &= \sqrt{\left( \frac{\partial H'}{\partial a} B a \right)^2 + \left( \frac{\partial H'}{\partial a} B_H \right)^2} \\ p_H &= \sqrt{\left( \frac{\partial H'}{\partial a} P a \right)^2 + \left( \frac{\partial H'}{\partial a} P_H \right)^2} \end{aligned} \right\} \quad (17)$$

For Pitch;

$$\left. \begin{aligned} P' &= \left( \frac{P}{\frac{360a}{\lambda}} \right) \\ B_{P''} &= \sqrt{\left( \frac{\partial P''}{\partial \lambda} B \lambda \right)^2 + \left( \frac{\partial P''}{\partial p} B p \right)^2 + \left( \frac{\partial P''}{\partial a} B a \right)^2} \\ p_{P''''} &= \sqrt{\left( \frac{\partial P''}{\partial \lambda} P \lambda \right)^2 + \left( \frac{\partial P''}{\partial p} P p \right)^2 + \left( \frac{\partial P''}{\partial a} P a \right)^2} \\ U_{P'} &= \sqrt{(B_{P'})^2 + (p_P)^2} \end{aligned} \right\} \quad (18)$$

Similarly, uncertainty in frequency of wave, roll RAO etc.. can be calculated. Overall uncertainty is given by

$$\left. \begin{aligned} U_H' &= \sqrt{(U_H)^2 + \left(\frac{\partial H'}{\partial \omega} U_{\dot{\omega}}\right)^2} \\ U_P' &= \sqrt{(U_P)^2 + \left(\frac{\partial P'}{\partial \omega} U_{\dot{\omega}}\right)^2} \end{aligned} \right\} \quad (19)$$

#### 4. Model details

Hull form details of Ro-Ro Passenger ship are given in Table 2 and hull form model developed is shown in Figs. 1(a)-1(c). Numerical analysis was carried out for different sets of wave frequencies and wave details as shown in Table 3. Figs. 2(a) and 2(b) shows, model developed for numerical analysis in ANSYS and MAXSURF. Ship is discretized into 6954 element with 7036 nodes and mesh type is triangular and quadrilateral cells as shown in Fig. 2(d). Fig. 2(c) shows co-ordinate system used throughout motion analysis.

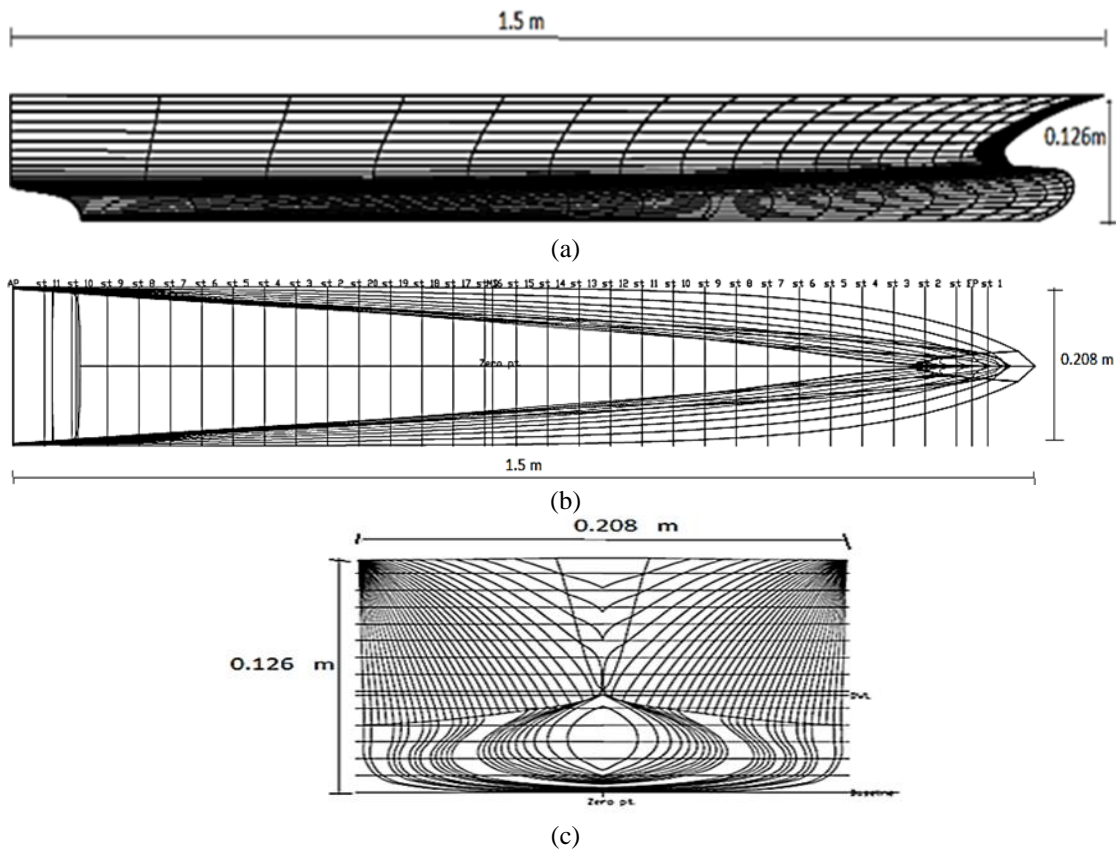


Fig. 1 Scale model of RO-RO Passenger Ship(a) Profile View, (b) Top View and (c) Front View

Table 2 Hull Form Properties of Ro-Ro vessel

Parameters	Unit	Dimensions
Displacement	N	164800
Volume (displaced)	m <sup>3</sup>	16391
Draft at AP	m	6.5
Block coefficient	-	0.561
Prismatic coefficient	-	0.604
Length overall	m	187
Length between perpendiculars	m	173
Breadth Moulded	m	26
Amidships section coefficient	-	0.929
Roll radius of gyration	m	-
Pitch radius of gyration	m	45.22
Depth to public spaces deck	m	15.7
Water plane coefficient	-	0.794
Height of metacenter above keel	m	14.08
Height of C.G above keel	m	11.04
Metacentric height	m	3.04
Longitudinal position of CG from AP	m	78.73

Table 3 Wave Conditions used by Korkut *et al.* (2004)

$\lambda/L_{pp}$	$\lambda$ (m)	T (s)	$\omega$	$\omega \sqrt{L_{pp}/g}$
2.9	4	1.6	3.9	1.52502068
2.4	3.33	1.45	4.3	1.681433057
2	2.79	1.35	4.7	1.837845434
1.65	2.28	1.2	5.2	2.033360906
0.9	1.26	0.9	7	2.737216605
0.72	0.99	0.8	7.9	3.089144454
0.48	0.66	0.65	9.7	3.793000152
0.41	0.57	0.6	10.4	4.066721812
0.28	0.39	0.5	12.6	4.926989888

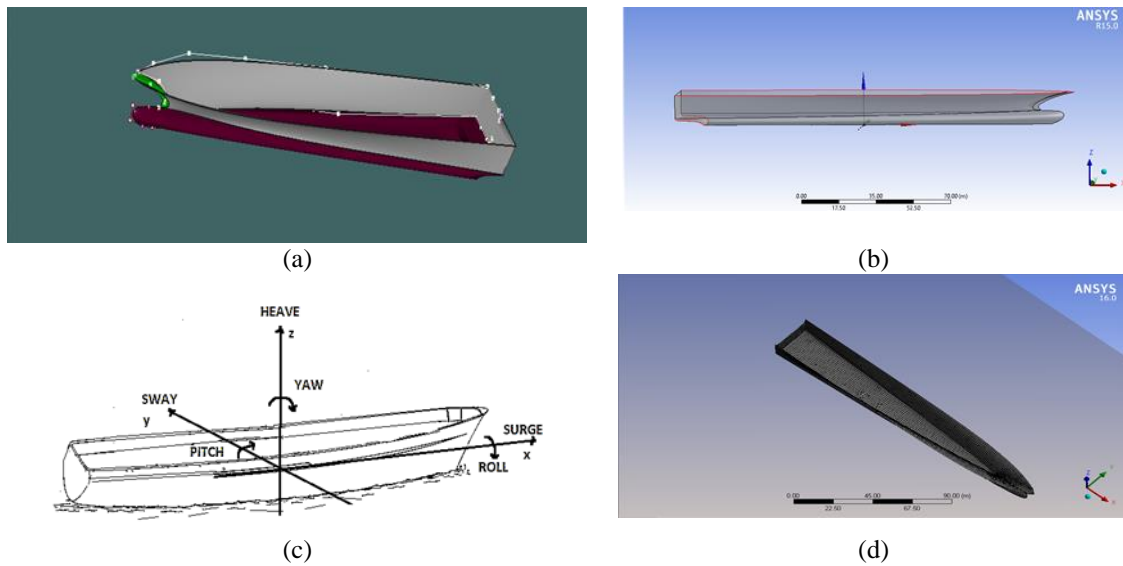


Fig. 2 Numerical model of Ro –Ro (a)Maxsurf Model, (b) ANSYS-AQWA Hydrodynamic Diffraction Analysis, (c) Co-ordinate system and (d) ANSYS-AQWA Mesh structure

### 5. Experimental investigation

A scaled model ratio of 1:125 was used for experimental studies at 40 x 2 x 2 m wave flume of National Institute of Technology Calicut. Hull model (Fig. 3) was developed using Fiber Reinforced polymer (FRP). Accuracy of hull form was ensured during fabrication as section planes were cut out from dies made for designed model in AutoCAD. Modelling was done using smooth spline curves (Fig. 1) which gives an accuracy up to 0.001 cm.



Fig. 3 Scale model for experimental investigation

Table 4 Error source for uncertainty analysis

Error Source	Error	Sensitivity	Error Component	
			Bias Limit	Precision Index
<b>MODEL DIMENSION</b>				
1) LBP	0.001 m	1	0.001 m	
2) B	0.001 m	1	0.001 m	
3) d	0.0002 m	1	0.0002 m	
<b>ACCELEROMETER</b>				
1) Linearity error	0.005 v	0.1 rad/volt	0.0005 rad	
<b>WAVE PROBE</b>				
1) Calibration Error	0.0003 m	0.15 m	0.00003 m	0.000045 m
2) Dynamic Error (B)	0.0002 m	0.15 m		
<b>MOTION SENSORS</b>				
1) Heave	0.002 m	0.21 m		0.00001 m
2) Roll	0.002 m	6 deg		0.002 deg
3) Pitch	0.002 m	6 deg		0.002 deg
<b>METACENTRIC HEIGHT</b>				
GMd (0.023 m)			0.002 m	0.00005 m

Uncertainty analysis is being performed to estimate error and accuracy of readings obtained. Error in model dimension is obtained during model manufacture. Displacement error gives us error in measurement of draft. Error in inclination experiment is due to unevenness in weight distribution in ship hull. This affect KG and GM values. Servo needle type wave probes are used to measure wave parameters. Calibration of measuring devices like motion sensors and wave plunger is done to estimate error sources (Table 4).

### 5.1 Inclination experiment

Metacentric height helps us to define stability of vessel. It puts limitations on quantity of load that vessel could carry at different stages of sea faring. Primary investigation of stability starts with Inclining test, where variation of angle of heel ' $\phi$ ' is found out when G shifts to G1 when a mass, 'm', is moved through a distance x. Metacentric height GM and displacement, ' $\Delta$ ', of ship in water are obtained by

$$GG_1 = GM \tan \phi \quad (20)$$

$$GG_1 = \frac{m \cdot x}{\Delta}, \quad GM = \frac{m \cdot x}{\Delta \tan \phi} \quad (21)$$

Above procedure is done using tilt sensor on model as shown in Table 5, at laboratory and results were obtained. In experiment conducted, mass, 'm', is 0.286 kg and  $\Delta$  is 8.6 kg. Fig. 4 shows stability curve obtained experimentally which is validated with numerically obtained GM value, which is 0.0229 m. An uncertainty of 0.0002 m is observed in experimental GZ plot (Fig. 4) which is considered to be insignificant for small angle of heel.

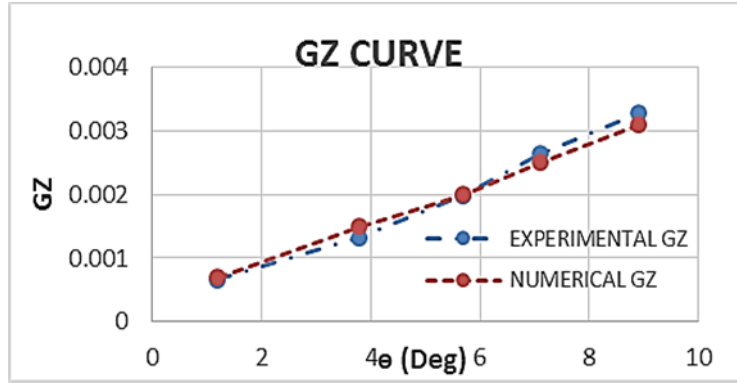


Fig. 4 Comparison of numerical and experimental GZ curve

Table 5 Experimental Observation and Calculation

x (m)	$\phi$ (deg)	$\phi$ (rad)	GM	GZ
0.02	1.2	0.020933333	0.031768429	0.000664971
0.04	3.8	0.066288889	0.020037801	0.001327311
0.06	5.7	0.099433333	0.020001024	0.001985493
0.08	7.1	0.123855556	0.021370436	0.002640085
0.1	8.9	0.155255556	0.021247665	0.003285581

### 5.2 Roll decay analysis

Prior to motion test, roll decay test was performed on ship to obtain natural frequency and time period in intact and damaged condition (Tables 6 and 8). Initially, vessel was held to a heel angle for 5s and then vessel is released. Model was heeled at an angle, and decay motion was generated. For initial heel angle of  $12^\circ$ , roll decay curve is obtained as shown in Figs. 5 and 6 at intact and damaged condition numerically. Damping coefficient of model was studied. Ship undergoes harmonic roll decay oscillation with a roll period  $T_{roll}$  and an initial roll angle  $\phi_0$ . A roll damping can be quantified by estimating decrement of successive wave’s roll amplitude (Xia 2002). Damping coefficient was obtained as shown in Table 7.

Table 6 Comparison of Natural Frequencies at Intact Condition

Parameters	Numerical			Experimental (Korkut <i>et al.</i> 2004)		
	H	R	P	H	R	P
Non-dimensional frequency	3.48	1.44	4.257	3.54	1.6	4.05
Ship Frequency of oscillation(rad)	0.8482	0.336	1.082	0.84	0.39	0.96
Ship period of oscillation(s)	7.4073	18.69	5.805	7.45	16.28	6.52

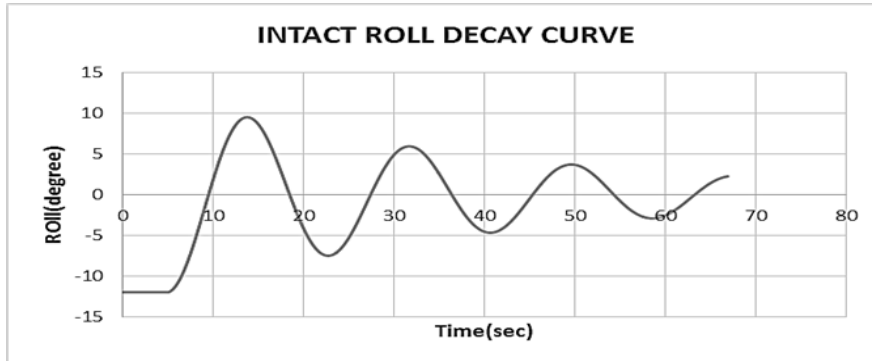


Fig. 5 Roll decay curve for intact model

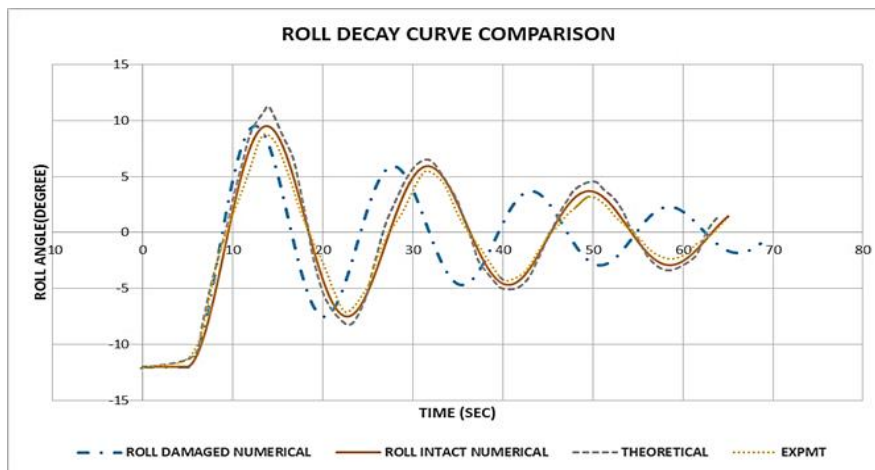


Fig. 6 Roll decay curve fitting

Table 7 Experimental and Numerical Damping Coefficient

Vessel Condition	Damping Coefficient
Intact	0.0030
Damaged	0.0022

Table 8 Comparison of Natural Frequencies at Damage Condition

Parameters	Numerical			Experimental (Korkut <i>et al.</i> 2004)		
	H	R	P	H	R	P
Non-dimensional frequency	3.918	1.9519	4.457	4.17	1.63	4.29
Ship Frequency of	1.0005	0.341	1.069	0.99	0.39	1.02
Ship period of oscillation(s)	6.28	18.424	5.877	6.33	16.03	6.15

H –Heave    R- Roll    P- Pitch

Using damping coefficient and period measured in roll decay test curve fitting is done as shown in Fig. 6. From Eq. (23), damping coefficient  $\delta$  can be computed depending on roll period  $T_{roll}$  and two consecutive roll angle maxima  $\phi_i$  and  $\phi_{i+1}$  (Molland 2008).

$$\varphi(t) = \varphi A e^{-\delta t} \cos \omega_0 t \quad (22)$$

$$\delta = \frac{1}{T_{roll}} \log_2 \sqrt{\frac{\phi_i}{\phi_{i+1}}} \quad (23)$$

Roll decay analysis was performed up-to 70s for which 3 oscillation was completed in 65 s (Fig. 5). In numerical roll decay analysis, a section of hull is considered to be damaged of size 0.043m to aft of hull. Opening is located 0.19 m from mid-section of hull. Roll decay under damaged condition is as shown in Fig. 6. Both in intact and damaged condition, curve show decay in roll amplitudes, although, after damage, decay of roll amplitude was faster and 3 oscillation was completed in 55s. Results were validated with that of Korkut *et al.* (2004). Ro-Ro vessels are designed to operate close to GM value at damaged condition. Hence damage roll decay response is considered important. Numerical study on roll decay at intact and damaged condition was done to understand damping coefficient, which is given in Table 7. Table 6 also shows that natural frequency of vessel in intact condition is 0.8482 while in damaged condition is 1.0005, which is close.

### 5.3 Motion analysis

Experimental investigations were carried out for wave conditions and testing environments in Wave flume at National Institute of Technology, Calicut (Figs. 7(a) and 7(b)). Hull was positioned 10 m from plunger and 10 m before beach in order to obtain uniform wave and to avoid reflection errors from tank walls. Heave response is measured using accelerometers and pitch responses using tilt sensors. Experiments were carried out for large wave heights ranging from 24.4 to 44 mm in flume, which is in range of 3.05 to 5.5 m in actual sea state condition. A series of tests were performed for regular waves.

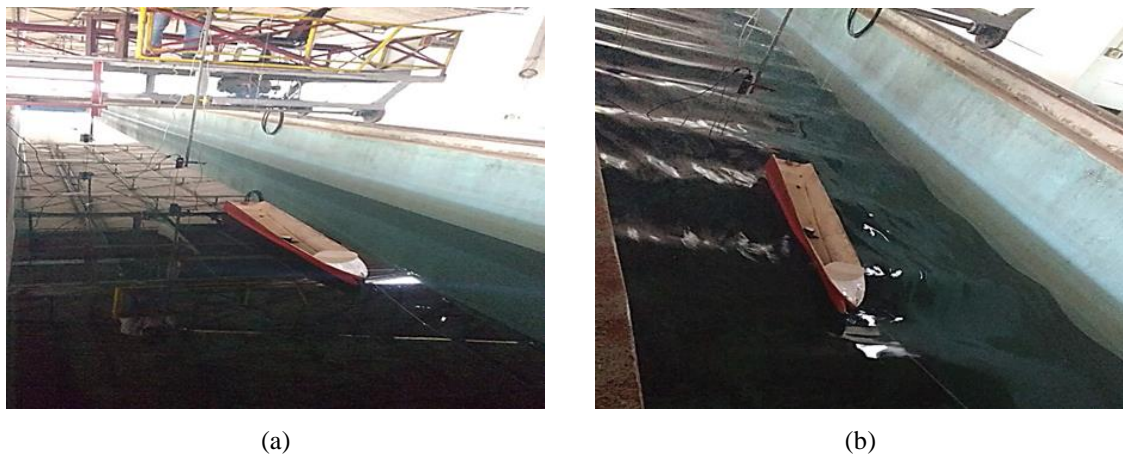


Fig.7 Head Sea condition (a) Without wave and (b) With wave

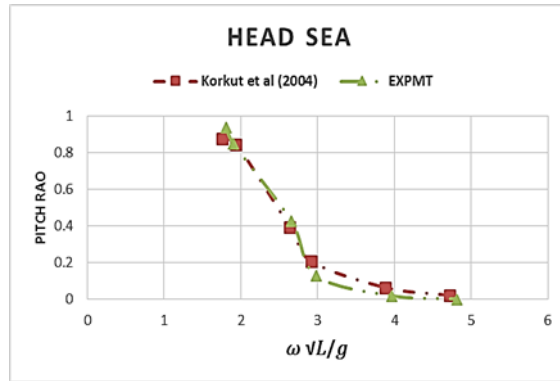


Fig. 8 The Pitch motion response of RO-RO Passenger Ship

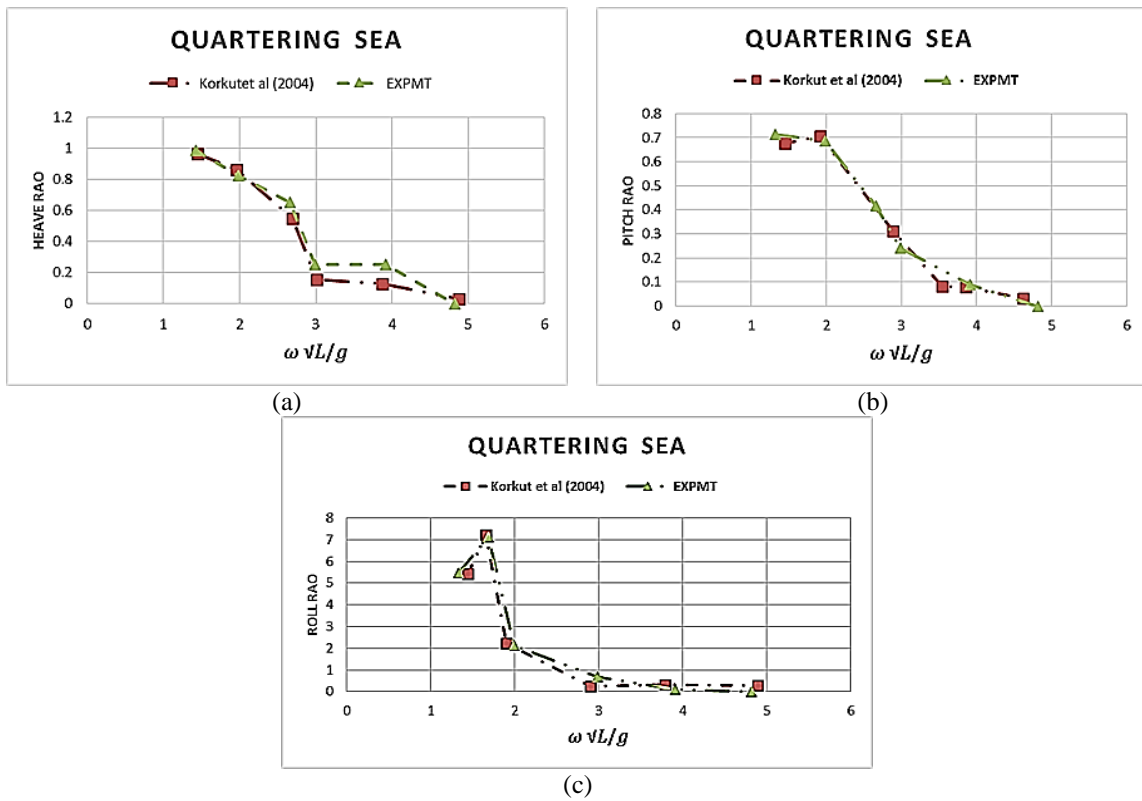


Fig. 9 The motion response of RO-RO Passenger Ship in quartering sea condition (a) Heave, (b) Pitch and (c) Roll

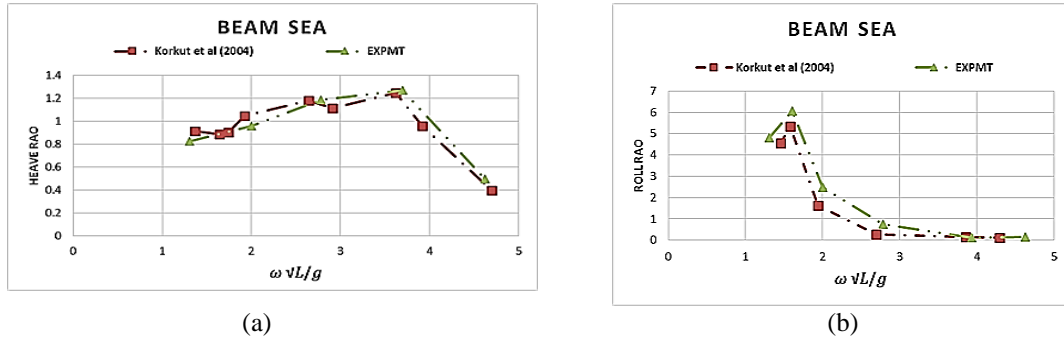


Fig. 10 The motion response of Ro-Ro Passenger Ship in Beam Sea condition (a) Heave and (b) Roll

Table 9 Uncertainty analysis of heave RAO in Quarter Sea

$\omega \sqrt{L_{pp}}/g$	$\lambda/L_{pp}$	H'	$U_H +$	$U_H + (%)$	$U_H - (%)$	$U_H - (%)$
1.525	2.9	0.963	0.0221	2.2126	0.0254	2.5421
1.681	2.4	0.963	0.0361	3.6126	0.0375	3.7514
1.837	2	0.963	0.0681	6.8126	0.0696	6.965
2.033	1.65	0.864	0.0097	0.9742	0.0099	0.999
2.737	0.9	0.549	0.1875	18.7563	0.1756	17.563
3.089	0.72	0.155	0.1154	11.5426	0.1234	12.344
3.793	0.48	0.212	0.0817	8.1763	0.0823	8.234
4.066	0.41	0.129	0.1856	18.5606	0.1883	18.834
4.926	0.28	0.0312	0.0937	9.37545	0.0778	7.785

Table 10 Uncertainty analysis of pitch RAO in Quarter Sea

$\omega \sqrt{L_{pp}}/g$	$\lambda/L_{pp}$	P'	$U_P +$	$U_P + (%)$	$U_P - (%)$	$U_P - (%)$
1.525	2.900	0.676	0.038	3.750	0.039	3.900
1.681	2.400	0.679	0.007	0.689	0.007	0.650
1.838	2.000	0.672	0.019	1.899	0.017	1.700
2.033	1.650	0.706	0.007	0.692	0.006	0.640
2.737	0.900	0.557	0.140	14.048	0.176	17.563
3.089	0.720	0.311	0.069	6.915	0.062	6.245
3.793	0.480	0.083	0.002	0.153	0.005	0.500
4.067	0.410	0.079	0.012	1.163	0.017	1.700
4.927	0.280	0.031	0.031	3.063	0.035	3.500

Data recording starts when wave reaches a steady state and is stopped when wave reaches wave absorber at other end of the wave flume. It is seen that peak responses occurs at a dimensionless

frequency of 1.5 which corresponds to resonance frequency as shown in Figs. 8-10. These results are used to validate the model developed.

On performing uncertainty analysis for quarter sea heave and pitch responses, it is found that nonlinearity occurs at a dimensionless frequency of 2.737. Uncertainty at this point is maximum of 14.05% in pitch response (Table 10) and 18.75% in case of heave response (Table 9). Similarly analysis was done for response RAO in head and beam sea conditions. The 95% confidence interval for pitch and heave RAO's was  $\pm 6\%$  and  $\pm 8\%$  respectively.

## 6. Numerical analysis

Numerical analysis is performed by considering a floating body which exhibits 6DOF based on which motion responses which are calculated in different wave directions (Korkut 2005). Translational and rotational responses of vessel in 6DOF are as shown in Fig. 2(f). The z-axis is directed upwards with encountering frequency  $\omega_e$  and wave frequency  $\omega$ . It was assumed that fluid is inviscid and incompressible. Strip theory is used which is based on potential flow theory.

Numerical results obtained using numerical code MAXSURF which is based on strip theory are shown in Figs. 11-13. A response peak is obtained for roll resonant condition for a non-dimensional frequency around 1.6 for both Beam (Fig. 13(b)) and Quartering condition (Fig. 12(c)). This is similar to roll decay frequency obtained in Table 5.

Heave response in quarter wave shows a nonlinearity or peak at dimensionless frequency around 4.07, which shows coupling of responses (Fig. 12(a)). This non linearity is visible in heave uncertainty analysis (Table 7) where uncertainty is 18.83% deviation from actual results. Numerical and experimental results of pitch response at head (Fig. 11) and quartering conditions (Fig. 12(b)) shows similar trends. A non-linearity is obtained in heave response under beam sea condition (Fig. 13(a)) at a non-dimensional frequency between 2.5 and 4 which is also confirmed with results in Table 5. Responses are also compared with ANSYS AQWA results which used Radiation/Diffraction theory to predict motion response. Motion response analysis results were found to lie close to experimental results in case of head and Quarter Sea while it was outside 95% confidence interval in case of Beam Sea.

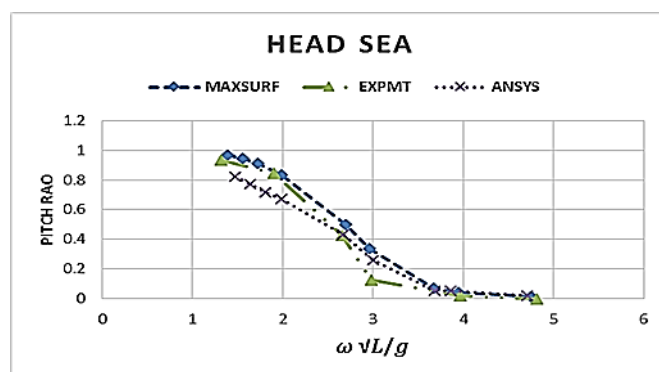


Fig. 11 The Pitch motion response of RO-RO Passenger Ship

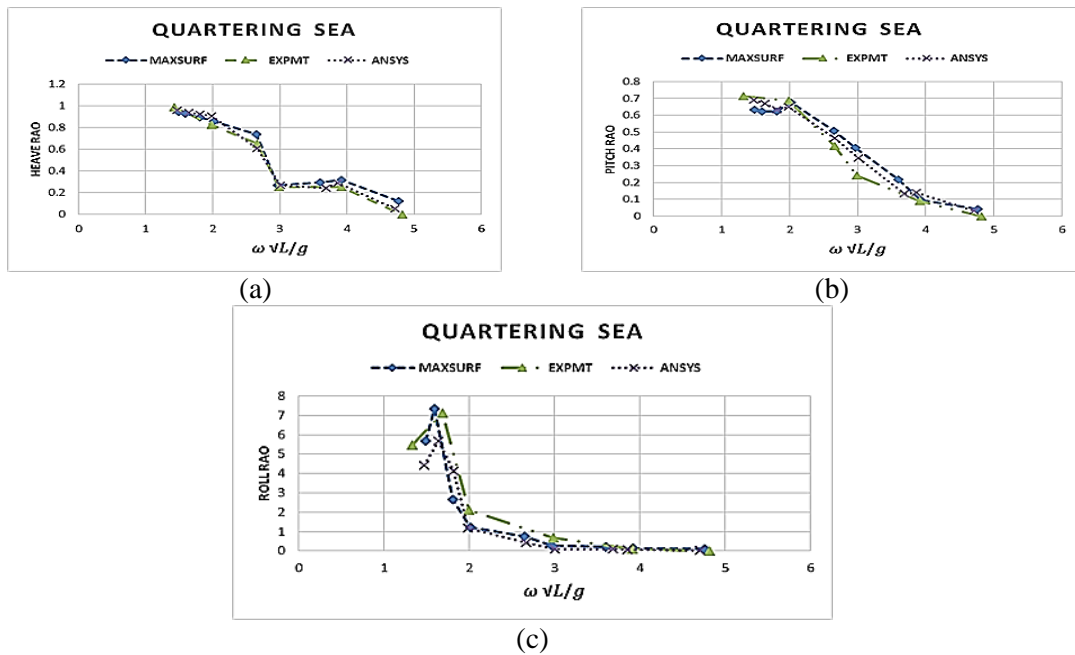


Fig. 12 Motion response of RO-RO Passenger Ship in quartering sea condition (a) Heave, (b) Pitch and (c) Roll

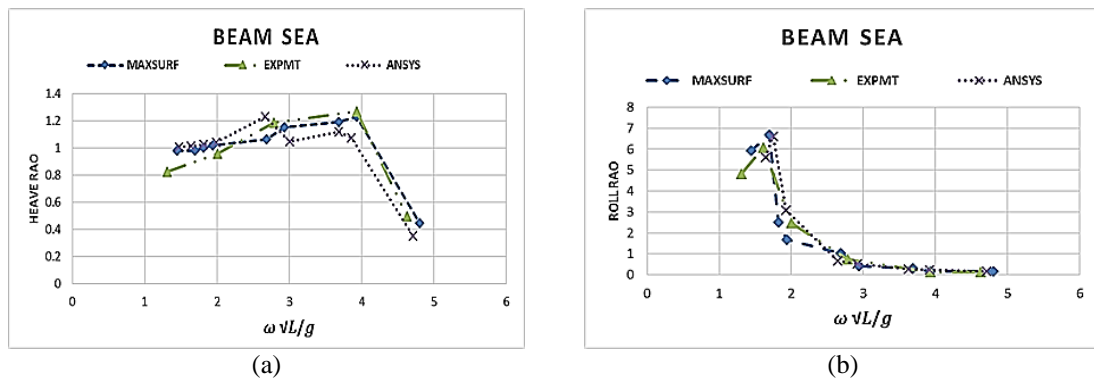


Fig. 13 Motion response of Ro-Ro Passenger Ship in Beam Sea condition (a) Heave and (b) Roll

It can be seen in Table 11 that roll response in quarter and Beam Sea shows greater uncertainty in the initial stages while compared to other responses. This occurs at dimensionless frequency range of 1.525 to 1.838. This is the point of resonance where the nonlinearity is observed in ship motion and stability assessment becomes difficult. Also the analysis results lies outside the uncertainty limits. In all other cases, the uncertainty is maximum at dimensionless frequency range of 2.737 to 3.089. The heave and pitch responses has a 95% confidence interval of  $\pm 8\%$ . Here the analysis results lies within the uncertainty limits.

Table 11 Overall percentage uncertainty (U %) of RAO

$\omega$ $\sqrt{L_{pp}/g}$	$\lambda/L_{pp}$	Quarter Heave	Quarter Pitch	Quarter Roll	Head Pitch	Beam Roll	Beam Heave
1.525	2.900	2.542	3.900	126.800	7.227	139.157	2.841
1.681	2.400	3.751	0.650	164.234	0.837	133.962	3.187
1.838	2.000	6.965	1.700	148.760	3.141	170.916	2.398
2.033	1.650	0.999	0.640	3.654	0.840	5.725	2.167
2.737	0.900	17.563	17.563	29.786	10.842	73.979	16.856
3.089	0.720	12.345	6.245	20.997	13.091	30.944	10.093
3.793	0.480	8.235	0.500	10.226	4.717	25.609	7.1826
4.067	0.410	18.834	1.700	7.700	2.399	3.9397	15.976
4.927	0.280	7.786	3.500	9.150	1.080	4.8122	9.708

## 7. Mathieu's equation of stability

Mathieu's equation of stability was developed to study parametric rolling condition. An elaborate study in parametric rolling was performed by many researchers. In-order to study primary stability characteristics of vessel under damped and undamped condition, theory described in Section 3.2 is utilized. Amplitude of this time dependent translation will vary, for a given natural frequency (Taylor *et al.* 1993). Here in this case, there are transition values of  $\alpha$  and  $\gamma$  for which Mathieu's equation has solutions that consist of  $2\pi$  or  $4\pi$  periodic solutions. Hence it is appropriate to assume a Fourier series representation of  $T=n\pi$  periodic solution to determine transition values of  $\alpha$  and  $\gamma$ . So, coefficient matrix for  $T=\pi, 2\pi, 3\pi, 4\pi$  was developed. For value of  $\alpha$  and  $\gamma$  around these values of  $T$ , the resonant condition is more probable to occur. It was utilized to code the Strutt –Ince diagram by equating determinant (Eqs. (23) and (24)) of matrix to zero. Corresponding MATLAB code was developed to study stability behavior of vessel. Many works were done by various researchers and undamped condition was found easy to be formulated. Undamped condition code was modified to incorporate damped condition. Mathieu's equation so formed is known as Damped Mathieu's equation. Moideen and Falzarano (2011) had also developed Strutt chart for damped Mathieu's equation which was compared (Fig. 14) with current code.

$$\begin{bmatrix} \alpha - \frac{1}{4} - \frac{\gamma}{2} & \frac{\mu}{2} & \frac{\gamma}{2} & 0 & 0 & 0 \\ -\frac{\mu}{2} & \alpha - \frac{1}{4} - \frac{\gamma}{2} & 0 & \frac{\gamma}{2} & 0 & 0 \\ \frac{\gamma}{2} & 0 & \alpha - \frac{9}{4} & \frac{3\mu}{2} & \frac{\gamma}{2} & 0 \\ 0 & \frac{\gamma}{2} & \frac{-3\mu}{2} & \alpha - \frac{9}{4} & 0 & \frac{\gamma}{2} \\ 0 & 0 & \frac{\gamma}{2} & 0 & \alpha - \frac{25}{4} & \frac{5\mu}{2} \\ 0 & 0 & 0 & \frac{\gamma}{2} & -\frac{5\mu}{2} & \alpha - \frac{25}{4} \end{bmatrix} = 0 \quad (23)$$

$$\begin{bmatrix} \alpha & \gamma/2 & 0 & 0 & 0 & 0 \\ \gamma & \alpha - 1 & \mu & \gamma/2 & 0 & 0 \\ 0 & -\mu & \alpha - 1 & 0 & \gamma/2 & 0 \\ 0 & \gamma/2 & 0 & \alpha - 4 & 0 & 0 \\ 0 & 0 & \gamma/2 & -2\mu & \alpha - 4 & 0 \\ 0 & 0 & 0 & \gamma/2 & 0 & 0 \end{bmatrix} = \mathbf{0} \quad (24)$$

Fig. 14 shows variation of stability region for different damping factor in comparison with work done by Moideen (2010). Further, the modified stability code was utilized to find the stability behaviour of Ro-Ro Vessel. Damping factor obtained in Table 7 was used as input parameter to obtain stability chart for Ro-Ro Vessel, as shown in Fig. 15.

Stability chart was developed based on Mathieu’s equation of stability. Ince-Strutt chart clearly captures variation of stability with damping. Analysis gives us an insight into roll motion and stability relationships.

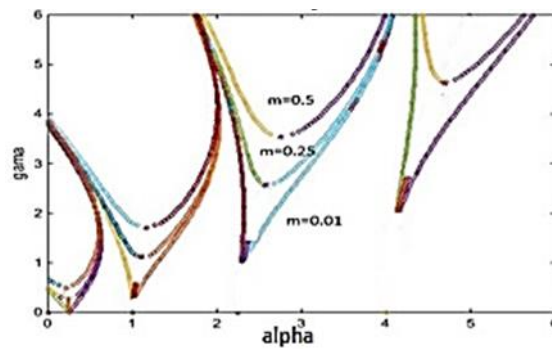


Fig. 14 Validation of the Strutt Chart

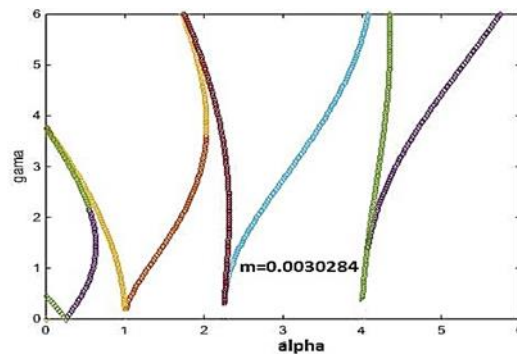


Fig. 15 Stability chart for RO-RO Vessel; m =0.003

## 8. Conclusions

The study aimed at developing a model to predict motion behaviour of Ro-Ro vessel and to bring out effect of damping in responses. The following conclusions are made:

1. Inclination test performed gave GM value 0.0229 m and roll decay test gave ships damping value 0.003. Uncertainty check was done for the same and error obtain was 0.0002 m in inclination test which is considered negligible. Curve fitting was done for roll decay curve and respective frequency of oscillation was obtained for heave, roll and pitch motion. The roll decay in damaged case showed a phase lag.
2. Ro-Ro vessel model is analyzed experimentally to understand motion behaviour and resonant non dimensionless frequency was obtained as 1.6. Uncertainty check is done. Overall uncertainty obtained was within limit for heave and pitch (+8%) responses while it was outside limit for roll responses as specified in ITTC recommended procedures for sea keeping experiments under different frequency ranges and for large wave height .
3. MATLAB code was developed for damped Mathieu's differential equation which gave Ince Strutt chart showing region of stability for Ro-Ro vessel under consideration. Stability chart is plotted to infer stability behaviour with a damping value of 0.003. Strutt chart can be further modified using Hill's Equation to obtain GM variations to reveal motion and stability characteristics of vessel.

## Acknowledgments

The authors would thank the support from TEQIP program in funding the experimental work conducted on wave flume at National Institute of Technology, Calicut.

## Funding

This research has received funding from the Technical Education Quality Improvement Programme (TEQIP phase II) at the National Institute of Technology, India.

## References

- Acanfora, M. and De Luca, F. (2016), "An experimental investigation into the influence of the damage openings on ship response", *Appl. Ocean Res.*, **58**, 62-70.
- Anastopoulos, P.A. and Spyrou, K.J. (2016), "Ship dynamic stability assessment based on realistic wave group excitations", *Ocean Eng.*, **120**, 256-263.
- Begovic, E., Mortola, G., Incecik, A. and Day, A.H. (2013), "Experimental assessment of intact and damaged ship motions in head, beam and quartering seas", *Ocean Eng.*, **72**, 209-226.
- Bergdahl, L. (2009), Wave-induced loads and ship motions, Department of Civil and Environmental Engineering, Division of Water Environment Technology, Chalmers University of Technology. Gothenburg, Sweden.
- Blome, T. and Krueger, S. (2003), "Dynamic stability of RoRo-Vessels in quartering waves", TU Hamburg-Harburg
- Fernández, R.P. (2015), "Stability investigation damaged ships", *J. Mar. Sci. Technol.* (Taiwan), **23**(4).

- Francescutto, A. (2015), "Intact stability criteria of ships - Past, present and future", *Ocean Eng.*, **120**, 312-317.
- Hanzu-Pazara, R., Arsenie, P., Duse, A. and Varsami, C. (2016), "Study of VLCC tanker ship damage stability during off-shore operation", *Proceedings of the IOP Conference Series: Materials Science and Engineering*, **145**. <http://doi.org/10.1088/1757-899X/145/8/082020>
- Hsiung, C.C. and Huang, Z.J. (1991), "Comparison of the strip theory and the panel method in computing ship motion with forward speed", *Proceedings of the Symposium on Selected Topics of Marine Hydrodynamics*, St. John's, Nfld.
- Ibrahim, R.A. and Grace, I.M. (2010), "Modeling of ship roll dynamics and its coupling with heave and pitch", *Math. Problem.Eng.*, Article ID 934714.
- Inspurger, T. and Stépán, G. (2003), "Stability of the damped mathieu equation with time delay", *J. Dyn. Syst. Meas. Control*, **125**(2), 166.
- Kerwin, J.E. (1995), "Notes on rolling in longitudinal waves", *Int. Shipbuild. Progress*, **2**(16), 597-614.
- Knapp, G.F. and Anderson, S.L. (1995), U.S. Patent No. 5,474,454. Washington, DC: U.S. Patent and Trademark Office.
- Korkut, E., Atlar, M. and Incecik, A. (2004), "An experimental study of motion behaviour with an intact and damaged Ro-Ro ship model", *Ocean Eng.*, **31**(3-4), 483-512.
- Korkut, E., Atlar, M. and Incecik, A. (2005), "An experimental study of global loads acting on an intact and damaged Ro-Ro ship model", *Ocean Eng.*, **32**(11-12), 1370-1403.
- Maxsurf Motions Program and User Manual (2015), Bentley Systems.
- Moideen, H. (2010), "Prediction of parametric roll of ships in regular and irregular sea", December, 148.
- Moideen, H. and Falzarano, J.M. (2011), "A critical assessment of ship parametric roll analysis", *Proceedings of the 11th International Ship Stability Workshop*.
- Molland, A.F. (2008), *The Maritime Engineering Reference Book*, Butterworth Heinemann.
- Ribeiro, J., Silva, E., Santos, T.A. and Guedes Soares, C. (2010), "On the parametric excitation of a container vessel", *Int. Shipbuild. Program.*, **52**, 29-56.
- Taylan, M. (2004), "Effect of forward speed on ship rolling and stability", *Math. Comput. Appl.*, **9**(2), 133-145.
- Taylor, R.E., Brown, D.T. and Patel, M.H. (1983), "Barge motions in random seas - a comparison of theory and experiment", *J. Fluid Mech.*, **129**, 385-407.
- Xia, J. and Fan, S. (2002), *Simulation of ship motions - coupled heave, pitch and roll*. centre for marine science and technology, Technical Report no. 35. WA: UWA.
- Zakaria, N.M.G. (2007), "Effect of ship size, forward speed and wave direction on relative wave height of container ships in rough seas", *IEM J.*, **70**(3), 21- 34.